Bull. Mater. Sci., Vol. 39, No. 7, December 2016, pp. 1835–1841. © Indian Academy of Sciences.
DOI 10.1007/s12034-016-1319-3

Theoretical study of built-in-polarization effect on relaxation time and mean free path of phonons in $Al_xGa_{1-x}N$ alloy

B K SAHOO and A PANSARI*
Department of Physics, National Institute of Technology, Raipur 492010, India

MS received 8 January 2015; accepted 25 April 2016

Abstract. **In this article we have investigated theoretically the effect of built-in-polarization field on various phonon scattering mechanisms in $Al_xGa_{1-x}N$ alloy. The built-in-polarization field of $Al_xGa_{1-x}N$ modifies the elastic constant, group velocity of phonons and Debye temperature. As a result, various phonon scattering mechanisms are changed. Important phonon scattering mechanisms such as normal scattering, Umklapp scattering, point defect scattering, dislocation scattering and phonon–electron scattering processes have been considered in the computation. The combined relaxation time due to above-mentioned scattering mechanisms has also been computed as a function of phonon frequency for various Al compositions at room temperature. It is found that combined relaxation time is enhanced due to built-in-polarization effect and makes phonon mean free path longer, which is required for higher optical, electrical and thermal transport processes. The result can be used to determine the effect of built-in-polarization field on optical and thermal properties of $Al_xGa_{1-x}N$ and will be useful, particularly, for improvement of thermoelectric performance of $Al_xGa_{1-x}N$ alloy through polarization engineering.**

Keywords. **$Al_xGa_{1-x}N$ alloy; built-in-polarization; phonon relaxation time; polarization engineering.**

1. Introduction

Wide-band-gap nitride semiconductors like $Al_xGa_{1-x}N$ are very promising materials for high-power and high-temperature applications in microwave communications, power electronics and optoelectronics [1]. By adjusting the Al composition, one can tune selected material properties such as band gap, lattice constant and polarization to the desired optimal value [2]. Recently, $Al_xGa_{1-x}N$ alloys, particularly Al-rich $Al_xGa_{1-x}N$ alloy, have attracted much interest due to their applications in solid-state UV light sources for bio-agent detection as well as for general lighting. The AlGaN/GaN high-electron-mobility transistors (HEMTs) have emerged as attractive candidates for high-voltage and high-power operation at microwave frequencies [3]. The material has a large peak electron velocity, large saturation velocity, high breakdown voltage and thermal stability, making this material very suitable for use as a channel material in microwave power devices [3,4]. $Al_xGa_{1-x}N$ is often used as a barrier layer, cladding layer or distributed Bragg reflector (DBR) in semiconductor lasers having quantum wells and taken as an active layer in short-wavelength (ultraviolet) light-emitting diodes (LEDs) and semiconductor lasers [5]. The performance of wurtzite nitride devices is reliable but affected by self-heating. The cause of self-heating is poor heat removal at the active region of the device. The heat removal from active region directly depends on thermal transport property of the material like thermal conductivity. Thus, properties of material that can enhance thermal transport should be explored so that high thermal conductivity as desired can be achieved. The high thermal conductivity can minimize the self-heating effect and can improve the performance of the nitride-based devices. Thermal management issues for miniaturised devices and their application for energy production through thermoelectric mechanisms require a thorough understanding of thermal parameters and processes governing thermal transport property of $Al_xGa_{1-x}N$ alloy [6–8].

The phonon scattering mechanism plays an important role in optical, electronic and thermal properties of the semiconductors and controls the design and efficiency of the optoelectronics devices [9,10]. To predict accurately the thermal, optical and electronic properties of $Al_xGa_{1-x}N$, one has to study in detail the phonon scattering processes in the material. On the other hand, the built-in-polarization effect, which is a unique and important phenomenon of $Al_xGa_{1-x}N$ alloy, is already known to influence the design and efficiency of the device [11–17]. These two internal fundamental phenomena independently or jointly influence the various properties of the $Al_xGa_{1-x}N$, whose net effect is observed at the device performance level. Recently, phonon–electron and phonon–phonon interactions have attracted interest in graphene and other technological important semiconductors [9,18–21]. Interestingly, these interactions are proposed and studied to explain some observations of fundamental phenomena. Some

*Author for correspondence (anjupansari20@gmail.com)

problems like intrinsic resistance, room temperature mobility and optical conductivity anomaly are thought to be resolved by examining the above-mentioned interactions. In case of $Al_xGa_{1-x}N$ light-emitting diodes and laser diodes, the self-heating and efficiency drop mechanism can be addressed by studying in detail the phonon scattering mechanism from various sources. The sources like impurities, defects and dislocations are inherent to the material; hence phonon scattering study from these sources may reveal the fundamental causes of loss mechanisms in light-emitting and laser diodes [22]. Liu and Balandin [23] have studied thermoelectric properties of $Al_xGa_{1-x}N$ and proposed that through phonon engineering the properties could be improved. Recently, Sztein *et al* [6–8] have theoretically calculated the thermoelectric properties. They have reported a method of improving thermoelectric performance through polarization engineering. Thermoelectric performance depends on electrical conductivity, thermal conductivity and Seeback coefficient. In their report, they have studied the built-in-polarization field effect on mobility and scattering mechanism of electrons and computed electrical conductivity and Seeback coefficient. However, to the best of author's knowledge, built-in-polarization field effect on phonon transport, phonon scattering mechanisms and on thermal transport has not been addressed [8].

In this work, we have examined the influence of built-in-polarization effect on various phonon scattering mechanisms and on their relaxation times in $Al_xGa_{1-x}N$ alloy. Various phonon scattering mechanisms like the Umklapp process, point defect scattering, dislocation scattering and phonon–electron scattering have been considered in the study. The interaction between the phonons and the built-in-polarization field and its effect on phonon relaxation time are fundamental in predicting the role of polarization mechanism in electronic, optical and thermal properties of $Al_xGa_{1-x}N$ for solar cells, LEDs and laser applications, and will be helpful for improvement of thermoelectric performance of $Al_xGa_{1-x}N$ alloy through polarization engineering.

2. The model

$Al_xGa_{1-x}N$/GaN heterostructures are of outstanding current interest for a wide range of device applications. In this structure, $Al_xGa_{1-x}N$ is the active material and the device performance is solely controlled by its properties. Typically $Al_xGa_{1-x}N$/GaN heterostructures are grown on a thick GaN template layer deposited on a sapphire substrate. Such heteroepitaxial growth typically gives rise to high strain inside the layers due to lattice mismatch. In the heterointerface, polarization charges are produced. This is due to difference in spontaneous polarization (sp) between GaN and $Al_xGa_{1-x}N$ ($P^{sp}_{AlGaN} - P^{sp}_{GaN}$), and induced piezoelectric polarization (P^{pz}) at the interface. In $Al_xGa_{1-x}N$ and GaN, spontaneous polarization P^{sp} originates due to non-centrosymmetric nature of their unit cell. Piezoelectric polarization (P^{pz}) charges arise due to strain produced by lattice mismatch between $Al_xGa_{1-x}N$ and GaN. The polarization charge density σ_p (polarization charge per unit area) at the heterojunction interface is given by [11]

$$\sigma_p = -2\left(e_{31} - e_{33}\left(\frac{C_{13}}{C_{33}}\right)\right)\left(\frac{a_{GaN} - a_{AlN}}{a_{AlN}}\right)x + P^{sp}_{GaN} - P^{sp}_{AlGaN},$$

where e_{31}, e_{33}, C_{13} and C_{33} are the relevant piezoelectric (pz) and elastic constants for $Al_xGa_{1-x}N$, a_{GaN} and a_{AlN} are the lattice constants of GaN and AlN, respectively, and P^{GaN}_{SP} and P^{AlGaN}_{SP} are the sp of GaN and $Al_xGa_{1-x}N$. These two polarizations form two-dimensional electron gas (2DEG) at the heterostructure interface. It has been shown from studies of $Al_xGa_{1-x}N$/GaN HFETs that polarization charges are a dominant factor in the formation of a 2DEG at the heterojunction interface. The expected 2DEG density n_s at the $Al_xGa_{1-x}N$/GaN heterojunction interface is given by [13]

$$n_s = \frac{\sigma_p}{e} - \frac{\varepsilon}{d\,e^2}(e\,\phi_s + E_F - \Delta E_c) + 0.5\,N_d\,d,$$

where ε is the dielectric constant of $Al_xGa_{1-x}N$, ϕ_s is the Schottky height of barrier (work function), E_F and ΔE_c are Fermi energy and conduction band offset, respectively, at the heterostructure interface, and d and N_d are the thickness (m) and donor concentration (m^{-3}), respectively, in the $Al_xGa_{1-x}N$ layer. The values of parameters of $Al_xGa_{1-x}N$ are $\varepsilon = x\varepsilon_{AlN} + (1-x)\varepsilon_{GaN}$, $\phi_b - \Delta E_c = 1.0$ eV, $E_F = 0.1$ eV, $N_d = 1 \times 10^{18}$ cm^{-3} and $d = 30$ nm. The approximate value of this 2DEG is about 10^{13} C cm^{-2}. The value of n_s has been obtained from Hall measurement [14].

This 2DEG forms an electric field F named as the built-in-polarization field present in the strained $Al_xGa_{1-x}N$ barrier layer, which approximately can be represented by $E(x) = (-9.5\,x - 2.1\,x^2)$ MV cm^{-1}. The strength of this electrostatic field depends on the $Al_xGa_{1-x}N$ alloy composition, strain, layer thickness, surface quality and the growth process. The intensity of this built-in-polarization field can reach several MV cm^{-1}. This field exists not only at the interfaces but also within the material film itself. These fields are a common feature of nitride heterostructures and have profound impact on nitride's optical, thermal and electrical properties. The direction of F depends on the polarity of the growth. Theoretical calculation indicates that the sp field is in the $[000\bar{1}]$ direction. For $Al_xGa_{1-x}N$ grown on GaN the strain is tensile, and results in a pz field in the $[000\bar{1}]$ direction. Thus, F is in the $[000\bar{1}]$ direction. This electric field can be determined by measuring potential drop across the AlGaN film. This field significantly influences the distribution and mobility of carriers; hence it has profound impact on optical, thermal and electrical properties of the heterostructures [3,8]. The role of built-in-polarization field in III–V nitride materials has been extensively studied for visible and ultraviolet light emitters, detectors, solar cells and high-power transistors. However, the role of this field with respect to their thermal transport properties has not been addressed. In this work, the main objective is to investigate the effect of built-in-polarization field on phonons and their scattering mechanisms, which are responsible for thermal transport properties of $Al_xGa_{1-x}N$/GaN heterostructures.

Recent work has demonstrated that polarization effects can exert a pronounced influence on heterostructure material properties and device physics, and furthermore that these effects can be used to achieve substantial improvements in various aspects of device performance [1]. The model is based on the fact that due to built-in-polarization field, the coupling between the elastic strain and electric field induces additional electric polarization. This additional polarization contributes to the elastic constant of the material [11]. If the elastic constant of AlGaN without consideration of polarization mechanism is C_{44}, then considering the polarization mechanism at the interface the elastic constant with polarization is [24,25] $C_{44,\mathrm{p}} = C_{44} + [(e_{15}^2 + e_{31}^2 + e_{33}^2 + P_{\mathrm{sp}}^2)/\varepsilon_0\varepsilon]$. This in turn modifies physical parameters such as phonon velocity, Debye temperature and Debye frequency of the material. Thermal conductivity is given by $k = 1/3\, C\, v\, l$, where C is specific heat, v is phonon velocity and l the phonon mean free path. Phonon mean free path is computed from phonon scattering mechanisms, which are functions of phonon velocity and Debye frequency. The computation of thermal conductivity requires a study of polarization effect on above-mentioned parameters. In this work we have studied the polarization effect on phonon scattering mechanisms.

In semiconductors, thermal energy is mostly carried by acoustic phonons. These phonons suffer scatterings from other phonons, electrons, impurities and defects due to which thermal energy is lost and hence thermal conductivity decreases. The scattering processes are split into normal scattering (τ_{N}) and resistive scattering (τ_{R}). The normal scattering process describes phonon–phonon scattering events where momentum is conserved and is given by [6]

$$\frac{1}{\tau_{\mathrm{N}}} = \frac{k_\beta\, \gamma^2\, V_0}{M\, \hbar^2\, v^5}\, \omega^2\, T^3, \tag{1}$$

where γ (=0.60) is the Gruneisen parameter, $V_0 = (\sqrt{3}/8)a^2c$ is the volume per atom, M is the molecular mass of AlGaN, v the velocity of phonons, T the temperature and ω the phonon frequency. Since phonon momentum is conserved in normal scattering, it does not directly limit thermal conductivity, but it does affect the phonon distribution in momentum and energy space. This modification of phonon distribution has an indirect impact on thermal conductivity and must be included. The resistive processes do not conserve phonon momentum and thus contribute directly to thermal conductivity. The resistive processes considered in this work are three-phonon Umklapp scattering (τ_{u}^{-1}), mass-difference scattering (τ_{m}^{-1}), dislocation scattering (τ_{d}^{-1}) and phonon–electron scattering ($\tau_{\mathrm{p-e}}^{-1}$). The Umklapp scattering describes phonon–phonon scattering events where momentum is not conserved. The scattering rate for Umklapp processes at $T = 300$ K and above is computed by the relation [26]

$$\frac{1}{\tau_{\mathrm{u}}} = 2\gamma^2 \frac{k_{\mathrm{b}} T \omega^2}{\mu V_0 \omega_{\mathrm{D}}}, \tag{2}$$

where $\mu = v_T^2 \rho$ is the shear modulus and ω_{D} the Debye frequency. The phonon scattering due to difference of masses of atoms is [26]

$$\frac{1}{\tau_{\mathrm{m}}} = \frac{V_0\, \Gamma \omega^4}{4\pi\, v^3}, \tag{3}$$

where $\Gamma = \sum_i f_i[1 - (M_i/\bar{M})]^2$ is the measure of the strength of the mass-difference scattering, f_i is the fractional concentration of the impurity atoms, M_i is the mass of the i^{th} impurity atoms and $\bar{M} = \sum_i\, f_i\, M_i$ is the average atomic mass. The phonon scattering rate at the core of the dislocation is proportional to the cube of the phonon frequency and is given by [27]

$$\frac{1}{\tau_{\mathrm{d}}} = \eta\, N_{\mathrm{D}} \frac{V_0^{4/3}}{v^2} \omega^3, \tag{4}$$

where N_{D} is the density of the dislocation lines of all types and $\eta = 0.55$ is the weight factor to account for the mutual orientation of the direction of the temperature gradient and the dislocation line. At low doping levels, the acoustic phonons scattered by electrons can be expressed as [26]

$$\frac{1}{\tau_{\mathrm{ph-e}}} = \frac{n_{\mathrm{e}} \varepsilon_1^2 \omega}{\rho v^2 k_\beta T} \sqrt{\frac{\pi\, m^* v^2}{2 k_\beta T}} \exp\left(- \frac{m^* v^2}{2 k_\beta T} \right), \tag{5}$$

where n_{e} is the concentration of conduction electrons, ε_1 is the deformation potential, ρ is the mass density and m^* is the electron effective mass. The resistive scattering rate can be written as a sum of Umklapp, mass difference, dislocation and phonon–electron scattering rates:

$$\frac{1}{\tau_{\mathrm{R}}} = \frac{1}{\tau_{\mathrm{u}}} + \frac{1}{\tau_{\mathrm{m}}} + \frac{1}{\tau_{\mathrm{d}}} + \frac{1}{\tau_{\mathrm{ph-e}}}. \tag{6}$$

According to the formulation of Klemen [28], the combined scattering rate can be written as a sum of the normal and resistive scattering rates:

$$\frac{1}{\tau_{\mathrm{c}}} = \frac{1}{\tau_{\mathrm{N}}} + \frac{1}{\tau_{\mathrm{R}}}. \tag{7}$$

The combined phonon relaxation time can be obtained by the summation of the inverse relaxation times of above-mentioned scattering processes and is given by [29]

$$\tau_{\mathrm{c}}^{-1} = \tau_{\mathrm{N}}^{-1} + \tau_{\mathrm{u}}^{-1} + \tau_{\mathrm{m}}^{-1} + \tau_{\mathrm{d}}^{-1} + \tau_{\mathrm{ph-e}}^{-1}. \tag{8}$$

The above-mentioned scattering model is applicable for room temperature and for low, medium and high doping level [3,4]. For validity of the scattering model a doping density of $10^{18}\,\mathrm{cm}^{-3}$ has been considered. This is the normal doping level in nitrides. In this work it has been assumed that even for low doping levels these formulas are valid. The doping level plays a significant role in phonon–electron scattering only and not in other scatterings. Hence change of doping level will modify only the phonon–electron scattering. The magnitude of other phonon scatterings will remain the same.

In this work the doping level of $10^{18}\,\mathrm{cm}^{-3}$ has been kept fixed for calculation of scattering mechanisms. The scattering mechanisms are computed at room temperature (300 K) as all devices operate at room temperature.

3. Result and discussion

First, material parameters of AlGaN alloy are computed. Generally, material parameters of an alloy are computed by Vegard's law [14]: $P_{\mathrm{AlGaN}}(x) = xP_{\mathrm{AlN}} + (1–x)P_{\mathrm{GaN}}$, where P stands for a physical parameter. The law is based on linear interpolation of binary values. It states that parameters depend linearly on composition. However, when composition varies, the impurities and alloys generate disorder in the material. These disorders introduce non-linearity (bowing) in the parameters. Hence, modified Vegard's law [11,14] $P_{\mathrm{AlGaN}}(x) = xP_{\mathrm{AlN}} + (1–x)P_{\mathrm{GaN}} + bx(1–x)$, where b is the bowing constant and needs to be employed for computation of material parameters of $Al_xGa_{1-x}N$ alloy. The bowing constant b expresses the degree of non-linearity. For lattice constants, band gap energy and elastic constants, the bowing constant b is known from first-principle calculations and experiments. However, bowing constant b is still unknown for a number of parameters. Investigation reveals that sp and pz polarizations of AlGaN alloy depend non-linearly on Al composition, i.e., they show a finite degree of bowing [11,14]. Thus, sp and pz polarizations strictly follow the modified Vegard's law. A number of experiments have validated this prediction [1]. The elastic constants are also composition-dependent parameters of the nitride alloys. This prediction has been validated by measuring surface acoustic wave velocity in $In_xGa_{1-x}N$ alloy by means of high-resolution Brillouin spectroscopy [1]. As polarization mechanisms contribute to elastic constants, the elastic constants would show more non-linear nature in the presence of polarization field than in its absence. For accurate prediction of optical and thermal properties of $Al_xGa_{1-x}N$/GaN heterostructure, bowing constant of elastic constant, phonon velocity and Debye temperature with and without polarization mechanism are required. In our earlier work we have computed these bowing constants by the method of best fit for elastic constant, phonon velocity and Debye frequency. The result is published elsewhere [25]. We directly use the result here.

The combined phonon relaxation time as a function of phonon frequency at room temperature has been calculated using equation (8) for different Al compositions. The phonon relaxation times, which are functions of phonon velocity and phonon frequency, are computed from phonon scatterings rates. These parameters in turn depend on Al compositions. Phonon velocity is computed from elastic constant of AlGaN by the relation $v = (C_{44}/\rho)^{1/2}$. The elastic constant of AlGaN without and with polarization is given by [25]

$$C_{44}^{\mathrm{AlGaN}} = x\,C_{44}^{\mathrm{AlN}} + (1-x)C_{44}^{\mathrm{GaN}} - 0.25\,x(1-x)\ \mathrm{GPa}, \tag{9}$$

$$C_{44,\mathrm{p}}^{\mathrm{AlGaN}} = x\,C_{44,\mathrm{p}}^{\mathrm{AlN}} + (1-x)C_{44,\mathrm{p}}^{\mathrm{GaN}} - 19.25x(1-x)\ \mathrm{GPa}. \tag{10}$$

It can be seen that bowing constant is higher in equation (10), which shows that polarization mechanism enhances the non-linearity property of the material parameter of $Al_xGa_{1-x}N$. The phonon velocity in $Al_xGa_{1-x}N$ as a function of Al composition without and with built-in-polarization mechanism can be written as [25]

$$v^{\mathrm{AlGaN}} = x\,v^{\mathrm{AlN}} + (1-x)\,v^{\mathrm{GaN}} - 1004.95\,x(1-x)\ \mathrm{m\,s^{-1}}, \tag{11}$$

$$v_{\mathrm{p}}^{\mathrm{AlGaN}} = x\,v_{\mathrm{p}}^{\mathrm{AlN}} + (1-x)\,v_{\mathrm{p}}^{\mathrm{GaN}} - 1496.60\,x(1-x)\ \mathrm{m\,s^{-1}}. \tag{12}$$

These expressions have taken bowing into account. Bowing arises due to built-in-polarization field in $Al_xGa_{1-x}N$ [16]. Debye frequency in $Al_xGa_{1-x}N$ is estimated as a function of Al composition with and without built-in-polarization. The Debye frequency without and with polarization can be expressed as [25]

$$\omega_{\mathrm{D}}^{\mathrm{AlGaN}} = x\,\omega_{\mathrm{D}}^{\mathrm{AlN}} + (1-x)\,\omega_{\mathrm{D}}^{\mathrm{GaN}} - 1.89559 \times 10^{13}\,x(1-x)\ \mathrm{rad\,s^{-1}}. \tag{13}$$

$$\omega_{\mathrm{D,p}}^{\mathrm{AlGaN}} = x\,\omega_{\mathrm{D,p}}^{\mathrm{AlN}} + (1-x)\,\omega_{\mathrm{D,p}}^{\mathrm{GaN}} - 2.81796 \times 10^{13}\,x(1-x)\ \mathrm{rad\,s^{-1}}. \tag{14}$$

The role of Al composition on various phonon scattering processes can be determined using these phonon velocity and Debye frequency expressions. This can give us idea of dependence of different properties of $Al_xGa_{1-x}N$ on Al composition. The normal scattering process has been calculated using equation (1). The Gruneisen parameter γ is choosen as 0.60 [7]. The volume per atom, V_0 (in unit cell of $Al_xGa_{1-x}N$), has been calculated using lattice constants of $Al_xGa_{1-x}N$ [14]. The molecular mass M of $Al_xGa_{1-x}N$ has been computed using Vegard's law [15]: $M_{\mathrm{AlGaN}} = xM_{\mathrm{AlN}} + (1-x)M_{\mathrm{GaN}}$. The temperature T is taken as room temperature (300 K) and ω is the phonon frequency. The scattering rate from Umklapp process has been computed using equation (2). It depends on Debye frequency, shear modulus and volume of unit cell. Debye frequency with and without built-in-polarization has been calculated using equations (13 and 14). The shear modulus has been computed using the relation $\mu = v^2\rho$, which is equal to the elastic constant of AlGaN. The phonon scattering rate due to the mass difference is calculated using equation (3). This scattering rate depends on volume of unit cell, the measure of the strength of the mass-difference scattering Γ, phonon frequency and phonon velocity. The strength of the mass-difference scattering Γ for $Al_xGa_{1-x}N$ is obtained from those of binary nitrides by

Vegard's rule [13]: $\Gamma_{AlGaN} = x\,\Gamma_{AlN} + (1-x)\Gamma_{GaN}$. The phonon scattering process due to dislocation is calculated using equation (4). This scattering process depends on phonons group velocity, phonon frequency and dislocation density N_D. The dislocation density N_D in AlGaN has been obtained by Vegard's rule [13]. The phonon–electron scattering process has been computed using equation (5). For AlN, the material parameters are $\Gamma = 3.2 \times 10^{-4}$, $N_D = 5.0 \times 10^{14}\,cm^{-2}$, $n_e = 5 \times 10^{15}\,cm^{-3}$, $\varepsilon_1 = 7.1\,eV$, $m^* = 0.14m_0$ and the material parameters for GaN are [10,29] $\Gamma = 1.3 \times 10^{-4}$, $N_D = 5.0 \times 10^{14}\,cm^{-2}$, $n_e = 3.3 \times 10^{15}\,cm^{-3}$, $\varepsilon_1 = 10.1$ eV and $m^* = 0.22m_0$. The material parameters such as carrier concentrations, dielectric constants and effective mass of $Al_xGa_{1-x}N$ have been obtained by Vegard's rule [30]: $n_e^{AlGaN} = x\,n_e^{AlN} + (1-x)\,n_e^{GaN}$, $\varepsilon_1^{AlGaN} = x\,\varepsilon_1^{AlN} + (1-x)\,\varepsilon_1^{GaN}$ and $m^{*AlGaN} = xm^{*AlN} + (1-x)\,m^{*GaN}$. The combined phonon relaxation time in $Al_xGa_{1-x}N$ as a function of phonon frequency at room temperature is shown in figure 1 for aluminum concentrations $x = 0$ and 0.2 with and without built-in-polarization field.

In figure 1, empty squares correspond to combined relaxation time without built-in-polarization field whereas filled squares represent relaxation time with built-in-polarization for Al concentration $x = 0$. The empty circles correspond to combined relaxation time without built-in-polarization while filled circles represent relaxation time with built-in-polarization for Al concentration $x = 0.2$. It can be observed from figure 1 that for $x = 0$, the combined relaxation time with built-in-polarization field is higher than that of the without polarization case at a given frequency. Thus phonon scattering rate is suppressed by built-in-polarization mechanism. These two curves ($x = 0$) correspond to phonon scattering with and without built-in-polarization field in GaN. The nature of the two curves ($x = 0$) is similar with respect to phonon frequency. The combined relaxation time of low-frequency phonons is significantly enhanced by the built-in-polarization phenomenon. However, as phonon frequency increases, this enhancement in relaxation time gradually decreases; hence the two curves come closer. Finally the two curves (with and without polarization) start overlapping, indicating that the combined relaxation time of high-frequency phonons is least influenced by built-in-polarization of the material [30]. Similar conclusions can be drawn for $x = 0.2$.

Figure 2 shows relaxation time of phonons in $Al_xGa_{1-x}N$ for higher Al concentrations. In figure 2, empty and filled stars correspond to combined relaxation time, respectively, without and with built-in-polarization for Al concentration $x = 0.4$. The empty and filled rhombus correspond to the combined relaxation time, respectively, without and with polarization for Al concentration $x = 0.6$. Finally the empty and filled triangles correspond to the combined relaxation time, respectively, without and with built-in-polarization field for Al concentration $x = 1$. Both figures 1 and 2 reveal that as the aluminum concentration increases the phonon relaxation time increases for both with and without built-in-polarization. However, it can be observed that the rate of increase is significantly higher in case of relaxation time with built-in-polarization field than relaxation time without built-in-polarization field [31]. This is due to lower atomic mass of Al than that of Ga atom and stronger built-in-polarization field in AlN in comparison with GaN. The former effect lowers scattering rates [10] and the latter effect suppresses phonon scattering rates [31]. The combined effect enhances the relaxation time of phonons for higher aluminium concentration. This shows that phonons move with a higher velocity and higher frequency in a medium with polarization field (strained medium) than in a medium of same length with no polarization field (unstrained medium). Thus phonons suffer less number of scatterings in a polarized medium. A noticeable change is expected in transport properties, particularly in phonon thermal conductivity and mobility of electrons

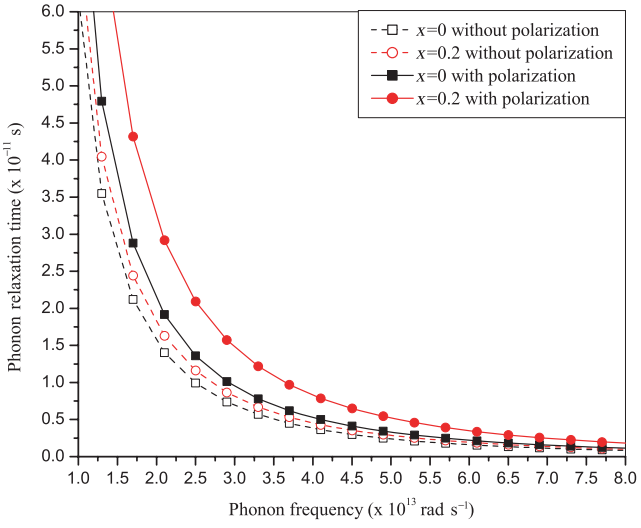

Figure 1. Combined relaxation times of phonons at room temperature for Al composition $x = 0$ and 0.2.

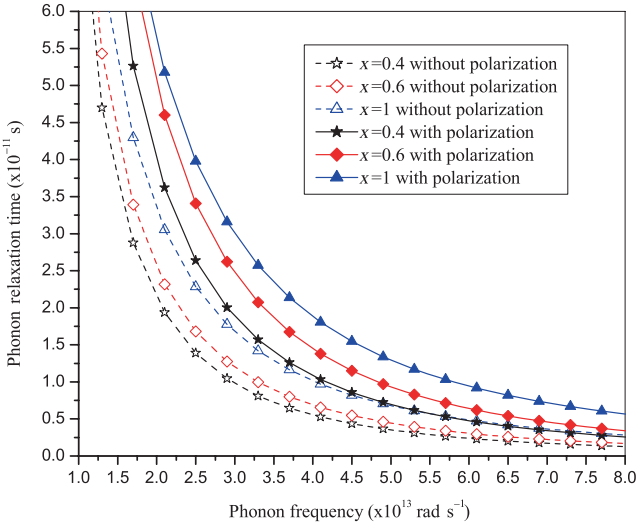

Figure 2. Combined relaxation times of phonons at room temperature for Al composition $x = 0.4$, 0.6 and 1.

in $Al_xGa_{1-x}N$, due to built-in-polarization property. Hence, high aluminium content $Al_xGa_{1-x}N$ can be chosen for design and fabrication of high-temperature and high-power HEMT for superior thermal and electrical performance [32].

For study of transport properties of semiconductors, phonon mean free path is very important. The phonon mean free path depends on its relaxation time. Hence, increased relaxation time will imply longer mean free path. This guarantees enhanced transport properties of the semiconductors. Thus, modifying the phonon relaxation time and mean free path of phonons in a controlled manner through polarization engineering, high transport properties, which are required for enhanced thermoelectric performance of $Al_xGa_{1-x}N$ for electric energy generation from waste heat energy through the Seebeck effect, can be achieved as required. It can resolve a number of issues relating to $Al_xGa_{1-x}N$ optoelectronics devices such as self-heating, switching action, etc. of HEMT. This gives the idea that by electrical means the phonon scattering processes can be controlled as and where desired. It can also increase the stability of devices at high temperature and high power.

4. Conclusions

In this work, the effects of built-in-polarization field on relaxation time and mean free path of phonons in $Al_xGa_{1-x}N$ alloy have been investigated theoretically. The relaxation time has been examined as a function of phonon velocity and Debye frequency. Using our previous result of phonon velocity and Debye frequency of $Al_xGa_{1-x}N$ alloy, it is found that the phonon scattering mechanism is suppressed, which happens due to polarization phenomenon. Our result shows that the combined relaxation time of low-frequency phonons is significantly enhanced by the polarization property; however, relaxation time of high-frequency phonons is the least modified. High aluminium concentration leads to enhanced phonon relaxation time, which implies longer phonon mean free path. A noticeable change is expected in transport properties, particularly in phonon thermal conductivity and mobility of electrons in $Al_xGa_{1-x}N$, due to the built-in-polarization property. Thus, by modifying the built in-polarization mechanism, transport properties in nitrides can be controlled. The phonon scattering mechanism, which is an important factor of design and performance of optoelectronic devices, can be modified in a controlled manner by judiciously tailoring the built-in-polarization property of material through polarization engineering. This result can be used for evaluating the built-in-polarization effect on thermal conductivity and thermoelectric performance of $Al_xGa_{1-x}N$ optoelectronics devices at room and high temperatures.

Acknowledgement

We thank Chhattisgarh Council of Science and Technology, Raipur, India, for providing financial support.

References

[1] Morkoc H 2013 *Nitride semiconductor devices* (Weinheim, Germany: Wiley-VCH Verlag GmbH & Co.)

[2] Lopuszy M and Majewski J A 2012 *J. Appl. Phys.* **111** 033502

[3] Morkoc H 2008 *Handbook of nitride semiconductors and devices* (Weinheim, Germany: Wiley-VCH Verlag GmbH & Co.)

[4] Piprek J 2007 *Nitride semiconductor devices: principles and simulation* (Weinheim, Germany: Wiley-VCH Verlag GmbH & Co.)

[5] Schubert E F 2006 *Light emitting diodes* (New York: Cambridge University Press)

[6] Sztein A, Bowers J E, DenBaars S P and Nakamura S 2012 *Appl. Phys. Lett.* **112** 083716

[7] Sztein A, Bowers J E, DenBaars S P and Nakamura S 2013 *Appl. Phys. Lett.* **113** 183707

[8] Sztein A, Bowers J E, DenBaars S P and Nakamura S 2014 *Appl. Phys. Lett.* **104** 042106

[9] Tanaka S, Matsunami M and Kimura S 2013 *Sci. Rep.* **3** 3031

[10] Alshaikhi A, Barman S and Srivastava G P 2010 *Phys. Rev. B* **81** 19530

[11] Wood C and Jena D 2000 *Polarization effects in semiconductors: from ab initio theory to device applications* (New York: Springer Science + Business Media) p 170

[12] Ambacher O, Smart J, Shealy J R, Weimann N, Chu K, Murphy M, Scaff W J, Eastman L F, Dimitrov R, Wittmer L, Stutzmann M, Rieger W and Hilsenbeck J 1999 *J. Appl. Phys.* **85** 3222

[13] Ambacher O, Foutz B, Smart J, Shealy J R, Weimann N, Chu K, Murphy M, Scaff W J, Eastman L F, Dimitrov R, Wittmer L, Stutzmann M, Rieger W and Hilsenbeck J 2000 *J. Appl. Phys.* **87** 334

[14] Ambacher O, Majewski J, Miskys C, Link A, Hermann M, Eickhoff M, Stutzmann M, Bernardini F, Fiorentini V, Tilak V, Schaff B and Eastman L F 2002 *J. Phys.: Condens. Matter* **14** 3399

[15] Bernardini F and Fiorentini V 2000 *Appl. Surf. Sci.* **166** 23

[16] Bernardini F, Fiorentini V and Ambacher O 2002 *Appl. Phys. Lett.* **80** 1204

[17] Bernardini F and Fiorentini V 2001 *Phys. Rev. B* **64** 08520

[18] Yan J, Zhang Y, Kim P and Pinczuk A 2007 *Phys. Rev. Lett.* **98** 166802

[19] Li Z Q, Henriksen E A, Jiang Z, Hao Z, Martin M C, Kim P, Stormer H L and Basov D N 2008 *Nat. Phys.* **4** 532

[20] Hwang E H and Das Sarma S 2008 *Phys. Rev. B* **77** 115449

[21] Siegel D A, Hwang C, Fedorov A V and Lanzara A 2012 *New J. Phys.* **14** 95006

[22] Verzellesi G, Saguatti D, Meneghini M, Bertazzi M, Goano M, Meneghesso G and Zanoni E 2013 *J. Appl. Phys.* **114** 071101

[23] Liu W and Balandin A A 2005 *J. Appl. Phys.* **97** 123705

[24] Sahoo B K, Sahoo S K and Sahoo S 2013 *J. Appl. Phys.* **114** 163501

[25] Pansari A, Gedam V and Sahoo B K 2015 *Physica B* **456** 66

[26] Zou J and Balandin A A 2001 *J. Appl. Phys.* **89** 2932

[27] Kotchetkov D, Zou J, Balandin A A, Florescu D I and Pollak F H 2001 *Appl. Phys. Lett.* **79** 43165

[28] Klemen P G 1997 In: *Chemistry and physics of nanostructures and related non-equilibrium materials* E Ma, B Fultz, R Shall, J Morral and P Nash (eds) (Warrendale: Minerals, Metals, and Materials Society)

[29] Florescu D I, Asnin V M, Pollak F H, Molnar R J and Wood C E C 2000 *J. Appl. Phys.* **88** 329

[30] Liu W and Balandin A A 2005 *J. Appl. Phys.* **97** 073710

[31] Gedam V, Pansari A, Sinha A K and Sahoo B K 2015 *J. Phys. Chem. Solids* **78** 59

[32] Gangwani P, Pandey S, Haldar S, Gupta M and Gupta R S 2007 *Solid-State Electron.* **51** 130